SOLAR DESIGN METHODS[1]

by
W. A. Beckman
University of Wisconsin-Madison

ABSTRACT

Design methods for solar thermal systems fall into two main categories. In the first are large, new, or one-of-a-kind systems which are best designed with the use of simulation methods. The detailed information that simulations provide is needed for new and unique kinds of systems, and the cost of doing simulations is small compared to the total costs involved in new or large systems.

The second category includes design of active systems that fit standard configurations, where adequate information on details of dynamics of performance is already available, and where the cost of the project does not warrant the expense of a simulation. Design procedures are available for many of these systems that are easy to use and provide adequate estimates of long-term thermal performance. In this chapter we briefly review some of these methods. The f-chart method, applicable to heating of buildings where the minimum temperature for energy delivery is approximately 20 C, is outlined in detail. Methods for designing systems delivering energy at other minimum temperatures, as are encountered solar absorption air conditioning or industrial process heat applications, are presented in Chapter 18 of Duffie and Beckman (1980).

1. REVIEW OF DESIGN METHODS

Design methods for solar thermal processes can be put in three general categories, according to the assumptions on which they are based and the ways in which the calculations are done. They all produce estimates of the long-term useful outputs of solar processes, but do not provide detailed information on process dynamics.

The first category applies to systems in which the collector operating temperature is known, and for which critical radiation level can be established (i.e., radiation levels above which useful energy can be collected). The first of these, the utilizability method, is based on analysis of hourly weather data to obtain the fraction of the total month's radiation that is above a critical level.

Another example in this category is the heat table method of R. Morse as described by Proctor (1975). This is a straightforward tabulation of integrated collector

[1] This paper is abstracted from Chapter 14 of "Solar Engineering of Thermal Processes," by J. A. Duffie and W. A. Beckman, Wiley-Interscience, NY, 1980.

performance as a function of collector characteristics, location, and orientation, assuming fixed fluid inlet temperatures.

The second category of design methods includes those that are correlations of the results of a large number of detailed simulations. The f-chart method of Klein et al. (1976, 1977) is an example. The results of many simulations are correlated in terms of easily calculated dimensionless variables. The results of the f-chart method have served as the basis for further correlations, e.g., by Ward (1976) who has used only January results, by Barley and Winn (1978) who used a 2 point curve fit to obtain location dependent annual results and by Lameiro and Bendt (1978) who also obtained location dependent annual results with 3 point curve fits.

Another example, in the second category is the method of Los Alamos Scientific Laboratory [Balcomb and Hedstrom (1976)], which is a correlation of the outputs of simulations for specific systems and two collector types.

The third category of design methods is based on short-cut simulations. In these methods, simulations are done using representative days of meteorological data and the results are related to longer term performance. The SOLCOST method [Connelly et al. (1976)] simulates a clear day and a cloudy day and then weights the results according to average cloudiness to obtain a monthly estimate of system performance.

2. THE f-CHART METHOD

This and the following sections outline the f-chart method for estimating the annual thermal performance of active heating systems for buildings (using either liquid or air as the working fluid) where the minimum temperature of energy delivery is 20 C. The system configurations that can be evaluated by the f-chart methods are expected to be common in residential applications. This material is present in more detail in *Solar Heating Design by the f-Chart Method* by Beckman et al.(1977).

The f-chart method provides a means for estimating the fraction of a total heating load that will be supplied by solar energy for a given solar heating system. The primary design variable is collector area; secondary variables are collector type, storage capacity, fluid flow-rates, and load and collector heat exchanger sizes. The method is a correlation of the results of many hundreds of thermal performance simulations of solar heating systems. The conditions of the simulations were varied over appropriate ranges of parameters of practical system designs. The resulting correlations give f, the fraction of the monthly heating load (for space heating and hot water) supplied by solar energy as a function of two dimensionless parameters, one related to the ratio of collector losses to heating loads and the other related to the ratio of absorbed solar radiation to heating loads.

The f-charts have been developed for three standard system configurations, liquid and air systems for space (and hot water) heating, and systems for service hot water only. A schematic diagram of the standard heating system using liquid heat transfer fluids is shown in Figure 1. This system normally uses an antifreeze solution in the collector loop and water as the storage medium. Collectors may be drained when energy is not being collected, in which case water is used directly in the collectors and a collector heat exchanger is not needed. A water-to-air load heat exchanger is used to transfer heat from the storage tank to a domestic hot water sub system. Although Figure 1 shows a two-tank domestic hot water system, a one-tank system could be used as described in Section 4. An auxiliary heater is provided to supply energy for the space heating load when it cannot be met from the tank. The ranges for major design variables used in developing the correlations are given in Table 1.

The standard configuration of a solar air heating system with a pebble bed storage unit is shown in Figure 2. Other equivalent arrangements of fans and dampers can be used to provide the same modes of operation. Energy required for domestic hot water is provided by an air-to- water heat exchanger in the hot air duct leaving the collector. During summer operation, it is best not to store solar energy in the pebble bed, so a manually operated storage bypass is usually provided in this system to allow summer water heating. The ranges of design parameters used in developing the correlations for this system are shown in Table 2.

The standard configuration for a solar domestic water heating system is shown in Figure 3. The collector may heat either air or liquid. The solar energy is transferred via a heat exchanger to a domestic hot water (DHW) preheat tank, which supplies solar heated water to a conventional water heater or an in-line low capacitance "zip" heater where the water is further heated to the desired temperature if necessary. A tempering valve may be provided to maintain the tap water below a maximum temperature. These changes in the system configuration do not have major effects on the performance of the system.

Detailed simulations of these systems have been used to develop correlations between dimensionless variables and f, the monthly fraction of loads carried by solar energy. The two dimensionless groups are

$$X = \frac{A_c F'_R U_L \left(T_{ref} - \bar{T}_a\right) \Delta\tau}{L} \tag{1}$$

$$Y = \frac{A_c F'_R \left(\overline{\tau\alpha}\right) \bar{H}_T N}{L} \tag{2}$$

where A_c = collector area (m^2)

F'_R = collector-heat exchanger efficiency factor[2]

U_L = collector overall loss coefficient (W/m^2 C)

Δt = total number of seconds in the month

$\bar{T}_a$ = monthly average ambient temperature (C)

[2] Although we indicate only a modification to F_R to account for the collector-storage heat exchanger, both $F_R(\tau\alpha)$ and $F_R U_L$ can be modified to account for the collector storage heat exchanger or duct losses or both.

T_{ref} = an empirically derived reference temperature (100 C)
L = monthly total heating load for space heating and hot water (J)
$\overline{H}_T$ = monthly average daily radiation incident on the collector surface per unit area (J/m^2)
N = days in month
$(\overline{\tau\alpha})$ = monthly average transmittance-absorptance product

The Equations 1 and 2 can be rewritten

$$X = F_R U_L \times \frac{F'_R}{F_R} \times \left(T_{ref} - \overline{T}_a\right) \times \Delta\tau \times \frac{A_c}{L} \tag{3}$$

$$Y = F_R(\tau\alpha)_n \times \frac{F'_R}{F_R} \times \frac{(\overline{\tau\alpha})}{(\tau\alpha)_n} \times \overline{H}_T N \times \frac{A_c}{L} \tag{4}$$

$F_R U_L$ and $F_R(\tau\alpha)_n$ are obtained from collector test results. F'_R/F_R corrects for various temperature drops between the collector and the storage tank and is given by de Winter (1975). $(\overline{\tau\alpha})/(\tau\alpha)_n$ can be approximated as a constant equal to 0.96 for one cover and 0.94 for two cover collectors. $\overline{T}_a$ is obtained from meteorological records for the month and location desired. $\overline{H}_T$ is found from the monthly average daily radiation on the surface of the collector. The monthly loads, L, are discussed in Section 3. A_c is the collector area. Thus, all of the terms in these two equations are readily determined from available information.

2. 1 Example

A solar heating system is to be designed for Madison, WI (latitude 43∞N), using one-cover collectors with $F_R(\tau\alpha)_n$ = 0.74 and $F_R U_L$ = 4.00 W/m^2 C as determined from standard collector tests. The collector is to face south with a slope of 60∞ from the horizontal. The average daily radiation on a 60∞ surface for January in Madison is 12.9 MJ/m^2 and the average ambient temperature is -7 C. The heating load is 36.0 GJ for space and hot water. The collector-heat exchanger correction factor, F'_R/F_R, is 0.97. The ratio of the monthly average to normal incidence transmittance-absorptance product $(\overline{\tau\alpha})(\tau\alpha)_n$, is 0.96 for the one-cover collectors with this orientation. Calculate X and Y for these conditions for collector areas of 25 and 50 m^2.

2.1.1 Solution

From Equations 3 and 4 with A_c = 25 m^2,

$$X = 4.0\ W/m^2\ C \times 0.97 \times [100 - (-7)]C$$
$$\times\ 31\ days \times 86400\ s/day \times 25\ m^2/36.0 \times 10^9 = 0.77$$
$$Y = 0.74 \times 0.97 \times 0.96 \times 12.9 \times 10^6\ J/m^2\ day$$
$$\times\ 31\ days \times 25\ m^2/36.0 \times 10^9\ J = 0.19$$

For 50 m^2, the values of X and Y are proportionally higher.

$$X = 0.77 \times 50/25 = 1.54$$
$$Y = 0.19 \times 50/25 = 0.38$$

As will be shown in later sections, the variables X and Y are used to determine f, the monthly fraction of the load supplied by solar energy. The energy contribution for the month is the product of f, and the total monthly heating load, L. The fraction of the annual heating load supplied by solar energy is the sum of the monthly solar energy contributions divided by the annual load

$$F = \frac{\Sigma f_i L_i}{\Sigma L_i} \qquad (5)$$

3. CALCULATION OF HEATING LOADS

A detailed discussion of heating and hot water loads is beyond the scope of this book, and for such a discussion the reader is referred to the ASHRAE Handbook of Fundamentals (1977). In this section we outline one method of estimating heating loads. The f-chart method is not dependent on the method used to calculate loads, and other means of estimating L can be used at the discretion of the designer.

The degree-day method of estimating loads is based on the principle that the energy requirement for space heating is primarily dependent on the difference in temperature between indoors and outdoors. The monthly space heating load for a building maintained at 24 C (75 F) is assumed to be proportional to the number of degree days in the month, DD,

$$L_s = (UA)_h DD \qquad (6)$$

where $(UA)_h$ is a loss coefficient-area product for the building. The number of degree-days is the difference between 18.3C and the mean daily ambient temperature, with positive values only included in the compilation. The difference between 24 C and 18.3 C allows for ordinary levels of internal energy generation in the building. Experience has shown that the fuel consumption for heating is approximately proportional to the number of degree-days. Long-term averages of degree-days by months are tabulated for many cities. (Recent trends toward lower thermostat settings as a means of reducing energy requirements and use of increased amounts of thermal insulation will lead to a reduction in the temperature base used in the definition of a degree-day.)

For existing structures where fuel consumption records are available, $(UA)_h$ may be calculated from

$$(UA)_h = \frac{(N_F H_F \eta_F)}{DD} \tag{7}$$

where N_F = units of fuel consumed
H_F = heating value of fuel consumed
η_F = efficiency of furnace

For new structures, $(UA)_h$ can be calculated from details of building construction by methods outlined in the ASHRAE Handbook of Fundamentals. From the design heating load and design temperature difference:

$$(UA)_h = \frac{\text{Design heating load}}{\text{Design temperature difference}} \tag{8}$$

Loads in the *f*-chart method may also include energy requirements for heating of hot water. The water heating loads are given by

$$L_w = C_p M(T_w - T_m) \tag{9}$$

where C_p = specific heat of water
M = hot water requirements for the month
T_w = set temperature for delivery of hot water
T_m = mains (supply) water temperature

Heat losses from the auxiliary hot water tank should be added to L_w, unless losses from that tank contribute to meeting the space heating loads in the winter. They can be estimated from $(UA)_{tank}(T_w - T_{room})$ or from manufacturers data.

3.1 Example

A residence in Madison has $(UA)_h$ = 463 W/C. It is expected that hot water requirements will be 450 kg/day, heated from 12 to 60 C. For the month of January, estimate the loads for space heating and hot water heating.

3.1.1 Solution

The Madison January degree days are 830 so the space heating load is

$$L_S = 463 \text{ x } 830 \text{ x } 24 \text{ x } 3600 = 33.2 \text{ G}$$

The water heating load is

$$L_W = 450 \text{ x } 31 \text{ x } 4190(60 - 12) = 2.8 \text{ GJ}$$

The total loads are 33.2 + 2.8 = 36.0 GJ for the month. (Note: heat losses from the auxiliary water heater are assumed to contribute to meeting the space heating load and are thus not included in the water heating load. In a summer month these losses would be added to L_W.

4. THE *f*-CHART FOR LIQUID SYSTEMS

The fraction, *f*, of the monthly total load supplied by the solar space and water heating system shown in Figure 4 is given as a function of X and Y in Figure 4. The relationship between X,Y, and *f* in equation form is

$$f = 1.029Y - 0.065X - 0.245Y^2 + 0.0018X^2 + 0.0215Y^3 \qquad (10)$$

Because of the nature of Equation 10, it should not be used outside of the range shown by the curves of Figure 4. If a calculated point falls outside of this range, the graph can be used for extrapolation with satisfactory results.

4.1 Example

The solar heating system described in Example 1 is to be a liquid system. What fraction of the annual heating load will be supplied by the solar energy for a collector area of 50 m^2? The monthly combined loads on the system are indicated in the table below.

4.1.1 Solution

From Example 1, the values of X and Y for 50m^2 are 1.54 and 0.38, respectively, in January. From Figure 4. (or Equation 10), $f = 0.26$. The total heating load for January is 36.0 GJ. Thus, the energy delivery from the solar heating system in January is

$$fL = 0.26 \text{ x } 36.0 \text{ GJ} = 9.4 \text{ GJ}$$

The fraction of the annual heating load supplied by solar energy is determined by repeating the calculation of X, Y, and *f* for each month, and summing the results as indicated by Equation 5. The table shows the results of these calculations. From Equation 5 the annual fraction of the load supplied by solar energy is

$$F = \frac{87.0}{203.2} = 0.43$$

Example 1. Monthly and Annual Performance of a Liquid Heating Systemin Madison, WI

Month	HT, MJ/m^2	$\overline{T_a}$	Load, GJ	$(\overline{\tau\alpha})/(\tau\alpha)_n$	X	Y	f	fL, GJ
Jan	12.9	-7	26.0	0.96	1.54	0.38	0.26	9.4
Feb	15.6	-6	30.4	0.94	1.64	0.48	0.34	10.3
Mar	16.0	0	26.7	0.93	1.95	0.62	0.43	11.5
Apr	14.5	7	15.7	0.92	2.99	0.92	0.57	8.9
May	15.4	13	9.2	0.90	4.92	1.68	0.86	7.9
Jun	16.2	19	4.1	0.89	9.96	3.79	1.00*	4.1
Jul	16.5	21	2.9	0.89	14.19	5.64	1.00*	2.9
Aug	16.5	20	3.4	0.92	12.25	4.97	1.00*	3.4
Sep	15.8	15	6.3	0.94	6.80	2.54	1.00	6.3
Oct	14.9	10	13.2	0.94	3.55	1.18	0.70	9.2
Nov	10.4	1	22.8	0.96	2.19	0.47	0.30	6.8
Dec	9.5	-5	32.5	0.96	1.68	0.31	0.19	6.2
Total			203.2					87.0

*These points have coordinates outside of the range of the *f*-Chart correlation.

To determine the economic optimum collector area, the annual load fraction corresponding to several different collector areas must be determined. The annual load fraction is then plotted as a function of collector area, as shown in Figure 5. The information in this figure can then be used for economic calculations.

For liquid systems, *f*-chart calculations can be modified to estimate changes in long-term performance due to changes in storage tank capacity and load heat exchanger characteristics. This is done by modifying the values of X or Y.

For liquid systems, *f*-chart calculations can be modified to estimate changes in long-term performance due to changes in storage tank capacity and load heat exchanger characteristics. This is done by modifying the values of X or Y as described below.

4.2 Storage Capacity

Annual system performance is relatively insensitive to storage capacity, as long as capacity is more than approximately 50 liters of water per square meter of collector. When the costs of storage are considered, there are broad optima in the range of 50 to 200 liters of water per square meter of collector.

The *f*-chart was developed for a storage capacity of 75 liters of stored water per square meter of collector area. The performance of systems with storage capacities in the range of 37.5 to 300 liters/m^2 can be determined by multiplying the dimensionless group X by a storage size correction factor, X_c/X, from Figure 6 or Equation 11.

$$\frac{X_c}{X} = \left(\frac{\text{Actual storage capacity}}{\text{Standard storage capacity}}\right)^{-0.25} \tag{11}$$

for

$$0.5 \leq \left(\frac{\text{Actual}}{\text{Standard}}\right) \leq 4.0$$

where the standard storage capacity is 75 liters of water per square meter of collector area.

4.3 Example

For the conditions of Example 10, what would be the annual solar contribution of the storage capacity of the tank is doubled, to 150 liters/m^2?

4.3.1 Solution

To account for changes in storage capacity, the value of X calculated in the previous examples must be modified using Figure 6 or Equation 11. The ratio of actual storage size to standard storage size is 2.0, so

$$\frac{X_c}{X} = (2.0)^{-1/4} = 0.84$$

For January the corrected value of X is then

$$X_c = 0.84 \times 1.54 = 1.29$$

The value of Y remains 0.38. From the *f*-chart, f = 0.28. The solar contribution for January is

$$fL = 0.28 \times 36.0 \text{ GJ} = 9.9 \text{ GJ}$$

Repeating these calculations for the remaining 11 months gives an annual solar load fraction of 0.45 (versus 0.43 for the standard storage size).

4.4 Load Heat Exchanger Size

As the heat exchanger used to heat the building air is reduced in size, the storage tank temperature must increase to supply the same amount of heat, resulting in higher collector temperatures and reduced collector output. A measure of the size of the heat exchanger needed for a specific building is provided by the dimensionless parameter, $\varepsilon_L C_{min}/(UA)_h$, where ε_L is the effectiveness of the water-air load heat exchanger and C_{min} is the minimum fluid capacitance rate (mass flow rate times the specific heat of the fluid) in the heat exchanger and is generally that of the air. $(UA)_h$ is the overall energy loss coefficient-area product for the building used in the degree-day space heating load model.

From thermal considerations, the optimum value of $\varepsilon_L C_{min}/(UA)_h$ is infinity. However, system performance is asymptotically dependent upon the value of this parameter, and for values of $\varepsilon_L C_{min}/(UA)_h$ greater than 10, performance will be essentially the same as that for the infinitely large value. The reduction in performance due to an undersized load heat exchanger will be significant for values of $\varepsilon_L C_{min}/(UA)_h$ less than about 1. Practical values of $\varepsilon_L C_{min}/(UA)_h$ are generally between 1 and 3 when the cost of the heat exchanger is considered. See Beckman et al. (1977) for further discussion.

The *f*-chart for liquid systems was developed with $\varepsilon_L C_{min}/(UA)_h = 2$. The performance of systems having other values of $\varepsilon_L C_{min}/(UA)_h$ can be estimated from the *f*-chart by modifying Y by a load heat exchanger correction factor, Y_c/Y, as indicated in Figure 7 or Equation 12.

$$\frac{Y_c}{Y} = 0.39 + 0.65e^{-\left(0.139(UA)_h/\varepsilon_L C_{min}\right)} \tag{12}$$

for

$$0.5 < \left(\frac{\varepsilon_L C_{min}}{(UA)_h}\right) < 50$$

4.5 Example

For the conditions of Example 10, what will be the solar contribution if the load heat exchanger is used under the following circumstances: air flow rate = 520 liters/s, water flow rate = 0.694 liters/s, and the heat exchanger effectiveness at these flowrates is 0.69. $(UA)_h$, the building overall energy loss coefficient-area product, is 463 W/C.

4.5.1 Solution

First, the value of C_{min} is determined. This usually the capacitance rate of the air, which in this example is

$$C_{min} = 520 \text{ liters/s} \times 1.20 \text{ kg/m}^3 \times 1010 \text{ J/kg C}/1000 \text{ liters/m} = 630 \text{ W/C}$$

The capacitance rate of the water is 2910 W/C so that of the air is lower. Then

$$\frac{\varepsilon_L C_{min}}{(UA)_h} = 0.69 \times \frac{(630 \text{ W/C}}{(463 \text{ W/C})}$$

$$= 0.94$$

This heat exchanger is smaller than the standard value of 2 used in developing Figure 4. The correction factor from Figure 6 or Equation 12 is

$$\frac{Y_c}{Y} = 0.95$$

$$Y_c = 0.95 \times 0.38 = 0.36$$

From Figure 4, $f = 0.24$ for January, and the solar energy contribution for the month is

$$fL = 0.24 \times 36.0 \text{ GJ} = 8.8 \text{ GJ}$$

The annual solar load fraction is found to be 0.41.

If both the storage and load heat exchanger sizes differ from the standards used to develop the f-chart, the correction factors discussed in Examples 11 and 12 would both be applied to find the appropriate values of X_c and Y_c for determination of f. Thus if the storage correction of Example 11 and the load heat exchanger correction of Example 12 are both needed, f would be determined at $X_c = 1.22$ and $Y_c = 0.33$ where $f = 0.24$.

5. THE f-CHART FOR AIR SYSTEMS

The monthly fraction of total heating load supplied by the solar air heating system shown in Figure 2 has been correlated with the same dimensionless parameters X and Y as were defined in Equations 1 and 2. The correlation is given in Figure 8 and Equation 13. It is used in the same manner as the f-chart for liquid-based systems. The equation is subject to the same cautions concerning the range of X and Y as the liquid system equations.

$$f = 1.040Y - 0.065X - 0.159Y^2 + 0.00187X^2 - 0.0095Y^3 \qquad (13)$$

5.1 Example

A solar heating system is to be designed for a building in Madison, WI with 2-cover collectors facing south at a slope of 58∞. The air heating collectors have the following characteristics: $F_R U_L = 2.84$ W/m^2 C and $F_R(\tau\alpha)_n = 0.49$. $(\overline{\tau\alpha})(\tau\alpha)_n = 0.93$ for this application of the two cover collector. The total space and water heating load for January is 36.0 GJ (as in Examples 10 to 12). What fraction of the load would be supplied by solar energy with a system having a collector area of 50 m^2?

5.1.1 Solution

For air systems, there will be no correction factor for the collector heat exchanger and we will assume duct losses are small, so that $F'_R/F_R = 1$. From Equations 3 and 4

$$Y = 0.49 \times 1 \times 0.93 \times (13.2 \times 10^6 \text{ J/day m}^2)$$

$$\times (31 \text{ days}) \times \frac{50 \text{ m}^2}{36.0 \times 10^9 \text{ J}}$$

$$= 0.259$$

Then f for January, from Figure 8 or Equation 13, is 0.19. The solar energy supplied by this system in January is

$$fL = 0.19 \times 36.0 \text{ GJ} = 6.8 \text{ GJ}$$

As with the liquid systems, the annual system performance is obtained by summing the energy quantities for all months. The result of the calculation is that 37% of the annual load is supplied by solar energy.

Air systems require two correction factors, one to account for effects of storage size if it is other than 0.25 m^3/m^2, and the other to account for air flow rate that affects stratification in the pebble bed. In addition, care must be exercised to be sure that the values of $F_R(\tau\alpha)_n$ and $F_R U_L$ from collector test are obtained for the same air flow rates as will be used in an installation. Corrections can be used to convert test data from one flow rate to another (see Duffie and Beckman (1980)). The correction factors for storage capacity and air flow rate are outlined below. There is no load heat exchanger in air systems.

5.2 Air Flow Rate

An increase in air flow rate tends to improve system performance by increasing F_R, and tends to decrease performance by reducing the thermal stratification in the pebble bed. The f-chart for air systems is based on a standard collector air flow rate of 10 liters/s of air per square meter of collector area. The performance of systems having other collector air flow rates can be estimated by using the appropriate values of F_R and Y and then modifying the value of X by a collector air flow rate correction factor X_c/X, as indicated in Figure 9 or Equation 14 to account for the degree of stratification in the pebble bed.

$$\frac{X_c}{X} \doteq \left(\frac{\text{Actual air flow rate}}{\text{Standard air flow rate}}\right)^{0.28} \tag{14}$$

for

$$0.5 < \left(\frac{\text{Actual}}{\text{Standard}}\right) < 2$$

where the standard air flow rate is 10 liters/s per square meter of collector area.

5.3 Example

The system of Example 13 is to be designed using a collector air flow rate of 15 liters/s per square meter of collector. Estimate the change in annual performance of the system resulting from the increased air flow.

5.3.1 Solution

Increasing the air flow rate affects F_R and stratification in the pebble bed. The effects of air flow rate on F_R and thus in F_RU_L and $F_R(\tau\alpha)_n$ must be determined either by collector tests at the correct air flow rate or estimated. In this case, $F_R(\tau\alpha)_n = 0.52$ and $F_RU_L = 3.01$ W/m^2 C at 15 liters/s m^2. The corrected X to account for pebble bed stratification if found from Equation 14 of Figure 9

$$\frac{X_c}{X} = \left(\frac{15}{10}\right)^{0.28} = 1.12$$

Thus the X to be used is the value from example 13 corrected for the modified F_R and for the air flow rate

$$X_c = 1.13 \times \frac{3.01}{2.84} \times 1.12 = 1.34$$

Correcting Y for the new value of F_R (i.e., $F_R(\tau\alpha)_n$)

$$Y_c = 0.259 \times \frac{0.52}{0.49} = 0.27$$

From the air f-chart, $f = 0.19$ and $fL = 6.8$ GJ for January. The calculation for the year indicates that 38% of the annual load is supplied by solar energy. (This is a slight increase over the 37% at the standard air flow rate; the increase must be evaluated in light of the increased fan power required at the higher air flow rate.)

5.4 Pebble Bed Storage Capacity

The performance of air systems is less sensitive to storage capacity than that of liquid systems. Air systems can operate in the collector-load mode, in which the storage unit is bypassed. Also, pebble beds are highly stratified and additional capacity is effectively added to the cold end of the bed, which is seldom heated and cooled to the same extent as the hot end.

The f-chart for air systems is for a storage capacity of 0.25 cubic meters of pebbles per square meter of collector area, which corresponds to 350kJ/m^2 C for typical void fractions and rock properties. The performance of systems with other storage capacities can be determined by modifying X by a storage size correction factor , X_c/X, as indicated in Figure 10 or Equation 15

$$\frac{X_c}{X} = \left(\frac{\text{Actual air flow rate}}{\text{Standard air flow rate}}\right)^{-0.30} \qquad (15)$$

for

$$0.5 < \left(\frac{\text{Actual}}{\text{Standard}}\right) < 4.0$$

where the standard storage capacity is 0.25 m^3/m^2.

5.5 Example

If the system of Example 13 has storage capacity which is 60 percent of the standard capacity, what fraction of the annual heating load would the system be expected to supply?

5.5.1 Solution

The storage size correction factor, from Figure 10 (or Equation 15), is 1.17. Then for January

$$\frac{X_c}{X} = 1.17$$

$$X_c = 1.17 \times 1.13 = 1.32$$

Y remains 0.26. From Figure 8 or Equation 15, f=0.18 and fL=0.18 x 36.0 GJ =6.5 GJ. The fraction of the annual load supplied by solar energy is 0.35 (compared to 0.37 for the standard storage size).

If both air flow rate and storage size are non standard, there will be two corrections on X to be made (in addition to any corrections due to changes in F_R) and the final X will be the product of the uncorrected value and the two correction factors.

If a phase-change energy storage unit is used in place of the rock bed, an empirical equation for the equivalent rock bed storage capacity is given by Duffie and Beckman (1980) which can be used to predict system performance. The properties and mass of the phase-change material are used to estimate the size of an equivalent rock bed, which is the used in the air f-chart correlations.

6. SERVICE WATER HEATING SYSTEMS

Figure 4, the f-chart for liquid heating systems, can be used to estimate the performance of solar water heating systems having the configuration shown in Figure 3, by defining an additional correction factor on X. The mains water supply temperature, T_m, and the minimum acceptable hot water temperature, T_w, both affect the performance of solar water heating systems. Both T_m and T_w affect the average system operating temperature level and thus the collector energy losses. The dimensionless group X, which is related to collector energy losses, can be corrected to include these effects. If monthly values of X are multiplied by a water heating correction factor, X_c/X in Equation 16 the f-chart for liquid-based solar space and water heating systems (Equation 10 or Figure 4) can be used to estimate monthly values of f for water heating systems. All temperatures are in C.

$$\frac{X_c}{X} = \frac{(11.6 + 1.8\,T_w + 3.86\,T_m - 2.32\,\bar{T}_a)}{(100 - \bar{T}_a)} \qquad (16)$$

This method of estimating water heater performance is based on storage capacity of 75 liters/m^2 and on the typical day's distribution of hot water use occurring each day. If other distributions of use occur, a system may not perform as well as indicated by the f-chart. Effect of storage size is difficult to predict and will depend on use patterns.

The water heating correction factor is based on the assumption of a wellinsulated solar preheat tank, and losses from an auxiliary tank were not included in the *f*-chart correlations. For systems supplying hot water only, loads on the system should also include losses from the auxiliary tank. (These are normally included in the energy supplied to a conventional water heater.) Tank losses can be estimated from the insulation and tank area, but this frequently leads to their underestimation as losses through connections, mounting brackets, etc. can be significant. It is recommended that tank loss calculations be based on the assumption that the entire tank is at the water set temperature, T_w.

The use of a tempering valve on the supply line to mix cold supply water with solar heated water above the water set temperature has little effect on the overall output of the solar system, and the method indicated here can be used for systems either with or without the tempering valve.

6.1 Example

A solar water heating system is to be designed for a residence in Madison, WI (latitude 43°N). The collectors considered for this purpose have two covers with $F'_R(\tau\alpha)_n = 0.64$ and $F'_R U_L = 3.64$ W/m^2 C. The collectors are to face south at a slope of 45°. The estimated water heating load is 400 liters/day heated from 11 C to 60 C. The storage capacity of the preheat tank is to be 75 liters of water per square meter of collector area. The auxiliary tank has a capacity of 225 liters, and has a loss coefficient of 0.62 W/m^{2}C. The tank is a cylinder 0.50 m diameter and 1.16 m high. Estimate the fraction of the January heating load supplied by solar energy for this system with a collector area of 10m^2. The radiation of the collector, $\overline{H}_T$, is 11.8 MJ/m^2 and $(\overline{\tau\alpha})/(\tau\alpha)_n$ is 0.94.

6.1.1 Solution

The monthly load is the energy required to heat the water from T_m to T_w plus the auxiliary tank losses. For January, the energy to heat the water is

$$400 \text{ Liters/day} \times 1 \text{ Kg/liter} \times \text{J/Kg C} \times (60-11) \text{ C}$$
$$\times\ 31 \text{ day} \times \text{GJ}/10^9\text{J} = 2.55 \text{ GJ}$$

The loss rate from the auxiliary tank is $UA(T_w - T'_a)$. The tank area is 2.21 m^2, so the loss rate for T'_a of 20 C is

$$0.62 \times 2.21(60 - 20) = 55 \text{ W}$$

Energy required to supply this loss for the month is

$$\frac{55 \times 31 \times 24 \times 3600}{10^9} = 0.15\text{GJ}$$

The total load to be used in calculation of X and Y is then

$$2.55 + 0.15 = 2.70 \text{ GJ}$$

We now calculate X_c and Y

$$X_c = X\left(\frac{X_c}{X}\right) = \frac{10 \times 3.64 \,.\, [100 - (-7)] \times 31 \times 24 \times 3600}{2.70 \times 10^9}$$

$$\times \frac{[11.6 + 1.18(60) + 3.86(11) - 2.37(-7)]}{[100 - (-7)]}$$

$$= 5.10$$

$$Y = 0.64 \times 0.94 \times 11.8 \times 10^6 \times 31 \times \frac{10}{2.70 \times 10^9} = 0.81$$

From Figure 4 or Equation 10, $f = 0.41$. This process can be repeated for each of the twelve months and the annual solar contribution estimated.

7. *f*-Chart RESULTS

In the original development of *f*-charts [Klein (1976)], it was necessary to make a number of assumptions about systems and their performance. Several of these are worth noting as they are useful in interpreting results obtained from this method.

First, all liquid storage tanks were assumed to be fully mixed, both for main storage tanks for liquid systems and preheat tanks for all water heating. This assumption tends to lead to conservative estimates of long-term performance by overestimating collector inlet temperature. Second, for reasons of economy in simulations, all days were considered symmetrical about solar noon. This also leads to conservative estimates of system outputs. For water heating only, it has been noted above that energy in water above the set temperature is not considered useful. Thus, the computations tend to be conservative in their predictions. On the other hand, it has been assumed that there are no leaks in systems; most air systems leak to some extent, and this will tend to degrade performance below predicted levels.

There are implicit assumptions in this method; systems are well-built, flow distribution to collectors is uniform, flow rates are as assumed, and the system configurations are close to those for which the correlations were developed. If these are not true, systems can not be expected to perform as estimated by the *f*-chart method.

The results obtained with *f*-chart have been compared to results of detailed simulations for a variety of locations. Agreement is generally to within a few percent.

Table 3 shows some of these results for a liquid house-heating system.

Agreement of monthly solar fractions is not nearly as good as annual fractions, and the f-chart method should be used to estimate annual performance only.

There are a few measured annual performance data on heating systems that can be compared to f-chart results. MIT House IV was 52 percent heated by solar energy over 2 years. f-chart estimates (based on measured meteorological conditions) indicates a solar fraction of 57 percent. (The system configuration is close to, but not the same as, the f-chart system.) CSU House II, the air system was supplied with 72 percent of its heat by solar energy; f-chart predicts 76 percent for the period.

A year long experimental study of solar domestic hot water systems at the U.S. National Bureau of Standards was done by Fanney (1979). The annual fraction of the total load (water draw-off plus auxiliary tank losses) supplied by solar from measurements and from f-chart predictions is given in Table 4. Although there are differences between measured and predicted performance, the results agree reasonably well.

8. PARALLEL SOLAR ENERGY-HEAT PUMP SYSTEMS

For the parallel solar energy-heat pump system shown in Figures 11 and 12, Anderson (1979) and Anderson et al. (1979) have developed a design method based on a combination of the "bin" method and the f-chart method. In the parallel mode of operation the solar system is the primary energy source and its operation is unaffected by the presence of a heat pump, that is, the heat hump system acts as the solar system auxiliary energy source. Consequently, the f-chart method can be used to determine the solar contribution to the heating load. The remaining portion of the load is met by a combination of the energy delivered by the heat pump and auxiliary energy. Although the performance of the heat pump is affected by the presence of the solar system, the Anderson et al. study observed that this interaction is small and can be neglected. This means that the only effect of the solar system on the heat pump is a reduction of the load that the heat pump will meet. The results of bin method calculations for a heat pump only system can then be modified to predict heat pump performance in the presence of a solar system.

A typical set of heat pump and load characteristics are shown in Figure 13 as a function of ambient temperature. When the ambient temperature is above the balance point, the heat pump can supply more energy, Q_{del}, than is needed by the load, Q_L. When the ambient temperature is below the balance point, auxiliary energy must be used in addition to the heat pump.

The bin method for estimating the monthly energy usage of a stand-alone heat pump system is described in ASHRAE (1976). The method uses long-term weather data to determine the number of hours in which the ambient temperatures were within 2.8 C (5 F) temperature ranges called bins. The number of hours in each temperature bin for a particular month can be used to estimate the monthly purchased energy. For example, suppose a month has 15 hr in a temperature bin centered around 10 C. To meet the load during this 15 hr, the system needs to run only 15 hr times the ratio of Q_L to Q_{del} or 15

(2.2/8.1) = 4.1 hr. In this 4.1 hr the energy required by the heat pump is 4.1 x 3.4 = 13.9 kW-hr (50 MJ). This calculation must be repeated for each temperature bin above the balance point.

At temperatures below the balance point the heat pump alone cannot meet the load and auxiliary energy must be used to make up the deficit. If 12 hr are in the bin centered around -10 C, the heat pump will run continuously for the 12 hr at a rate of 2.1 kW for a total electrical requirement of 2.1 x 12 = 25.2 kW-hr (91 MJ). In addition, auxiliary energy must make up the difference between the load of 7.7 kW times 12 hr and the delivered energy of 4.6 kW times 12 hr, or 37.2 kW-hr (134 MJ). By repeated application of these calculations, the monthly purchased energy can be estimated from which annual values can be calculated.

For a house with a parallel solar-heat pump system in Columbia, MO the combined system performance is shown in Figure 14 as a function of collector area. For zero collector area the system is a stand-alone heat pump and the fraction of the load supplied by non purchased energy from the air is $FATM_0$. At any finite collector area, some energy is supplied by solar and some is from the ambient air. The design procedure assumes that on a monthly basis

$$FATM = FATM_0(1 - f) \tag{17}$$

where f is the monthly fraction by solar. This equation is a result of assuming that the only effect of the solar system on the heat pump performance is a reduction in the load.

With monthly results from f-chart, a bin method calculation, and Equation 17, the monthly fraction of the load supplied by non purchased energy can be estimated. The remainder of the load is supplied by a combination of compressor work supplied to the heat pump and auxiliary energy. If the auxiliary energy is electricity, there is no need to separate the purchased energy into fractions by compressor work and by auxiliary. However, if the auxiliary is not electricity, it is necessary to know each of the two fractions to do an economic assessment. Equation 18 is recommended by Anderson et al. to find the work fraction

$$FW = FW_0(1 - f) \tag{18}$$

where FW_0 is the work fraction for the stand alone heat pump. The auxiliary fraction is then

$$FAUX = (1 - FATM_0 - FW_0)(1 - f) \tag{19}$$

The results of using the design procedure given by Equations 17 through 19 have been compared to detailed computer simulations and typical results are shown in Figure 11. In this figure the fraction of the total load by purchased energy calculated by the two methods compare very well. A similar conclusion can be made concerning the work fraction, the fraction from the atmosphere and the fraction by solar.

9. SUMMARY

The f-chart method provides a means of quickly estimating the long-term performance of solar heating systems of standard configurations. The data needed are monthly average radiation and temperature, the collector parameters available from standard collector tests, and estimates of loads.

It should be recognized that there are uncertainties in the estimates obtained from the f-chart procedure. The major uncertainties arise from several sources. First, the meteorological data can be in error by as much as 5 to 10 percent, particularly when the horizontal data are converted to radiation on the plane of the collector. Second, average data are used in the calculations, and any particular year may vary widely form that average. Third, it is extremely difficult to predict what building heating loads will be as it is dependent on the habits of the occupants. Fourth, systems must be carefully engineered and constructed, with minimal heat losses, leakage, and other mechanical and thermal problems. Finally, (and probably least important), there are some differences between the f-chart correlation and individual data points.

It is difficult to quantitatively assess the impacts of these uncertainties on the results obtained from the method. However, two generalizations can be made. First, the relative effects of design changes can be established. For example, the effects on annual performance of a change in plate absorptance and emittance can be shown. The second decimal place is significant in this context. Second, the method will predict the performance of a given system, but because of the uncertainties only the first decimal should be considered as significant.

The calculation of the f-chart method can easily be done by hand, but they can be tedious. The method has been programmed, in combination with life cycle economic analysis, in an available program FCHART (1978).

10. REFERENCES

Anderson, J. V., M. S. thesis, University of Wisconsin-Madison (1979). "Procedures for Predicting the Performance of Air-to-Air Heat Pumps in Stand-Alone and Parallel Solar-Heat Pump Systems."

Anderson, J. V., J. W. Mitchell, and W. A. Beckman, Paper at Int'l Solar Energy Society Meeting, Atlanta (1979). "A Design Method for Parallel Solar-Heat Pump Systems."

ASHRAE *Systems Handbook*, American Society of Heating, Refrigeration, and Air Conditioning Engineers, NY (1976).

ASHRAE *Handbook of Fundamentals*, American Society of Heating, Refrigeration, and Air Conditioning Engineers, NY (1977).

Balcomb, J. D. and J. C. Hedstrom, *Proc. of the Int'l Solar Energy Society Conf.*, Winnipeg, 4, 281 (1976). "A Simplified Method for Sizing a Solar Collector Array for Space Heating."

Barley, C. D. and C. B. Winn, *Solar Energy*, 21, 279 (1978). "Optimal Sizing of Solar Collectors by the Method of Relative Areas."

Beckman, W. A., S. A. Klein, and J. A. Duffie, *Solar Heating Design by the f-chart*

Method, Wiley-Interscience, New York (1977).

Connelly, M., R. Giellis, G. Jenson, and R. McMordie, *Proc. of the Int'l Solar Energy Society Conference*, Winnipeg, 10 220 (1976). "Solar Heating and Cooling COmputer ANalysis--A Simplified Sizing Method for Non-Thermal Specialists."

deWinter, F., *Solar Energy* 17, 335 (1975). "Heat Exchanger Penalties in Double-Loop Solar Water Heaters."

Duffie, J. A. and W. A. Beckman, *Solar Engineering of Thermal Processes,* Wiley Interscience, New York (1980)

Fanney, A. H., Personal Communication on the National Bureau of Standards Solar Domestic Hot Water Test Facility (1979).

FCHART Users Manual, University of Wisconsin Engineering Experiment Station, Report 49 (1978).

Klein, S. A., W. A. Beckman, and J. A. Duffie, *Solar Energy,*18, 113 (1976). "A Design Procedure for Solar Heating Systems."

Klein, S. A., W. A. Beckman, and J. A. Duffie, *Solar Energy,*19, 509 (1977). "A Design Procedure for Solar Heating Systems."

Lameiro, G. AND P. Bendt, *Proc. of the 1978 Meeting of the American Section of the Int'l Solar Energy Society*, Denver, 2 (1), 113 (1978). "The GFL Method for Designing Solar Energy Space Heating and Domestic Hot Water Systems."

Proctor, D., Int'l Solar Energy Society Meeting, Los Angeles (1975). "Methods of Predicting the Heat Production of Solar Collectors for System Design."

Ward, J. C., *Proc. of the Int'l Solar Energy Society Conf.*, Winnipeg, 4, 336 (1976). "Minimum-Cost Sizing of Solar Heating Systems."

Table 1. Ranges of Design Parameters Used in Developing the *f*-Charts for Liquid Systems[a]

$0.6 \leq (\tau\alpha)_n$	≤ 0.9
$5 \leq F'_R A$	$\leq 120\ m^2$
$2.1 \leq U_L$	$\leq 8.3\ W/m^2C$
$30 \leq b$	≤ 90 deg
$83 \leq (UA)_h$	≤ 667 W/C

[a]From Klein et al. (1976).

Table 2. Ranges of Design Parameters Used in Developing the *f*-Charts for Air Systems[a]

$0.6 \leq (\tau\alpha)n$	≤ 0.9
$5 \leq F'_R A$	$\leq 120\ m^2$
$2.1 \leq U_L$	$\leq 8.3\ W/m^2C$
$30 \leq b$	≤ 90 deg
$83 \leq (UA)_h$	$\leq W/C$

[a]From Klein et al. (1976).

Table 3. Comparisons of Annual Fractions Met by Solar Energy, for *f*-chart and Detailed Simulations

Location	f-Chart	Simulation
Albuquerque, NM	0.64	0.64
Bismark, MD	0.68	0.69
Blue Hill, MA	0.71	0.74
Charleston, SC	0.71	0.70
Dodge City, KA	0.70	0.68
Madison, WI	0.65	0.67
Medford, OR	0.69	0.74
New York, NY	0.55	0.55
Phoenix, AZ	0.67	0.70
Santa Maria, CA	0.49	0.51
Seattle, WA	0.65	0.73

Table 4. Measured and Predicted Values of Annual Solar Fraction

Number of Tanks	Type	Heat Exchanger	Measured	Predicted
1	Liquid	External	0.36	0.37
2	Liquid	External	0.37	0.40
1	Liquid	Internal	0.45	0.43
2	Liquid	Internal	0.33	0.30
1	Air	External	0.20	0.21

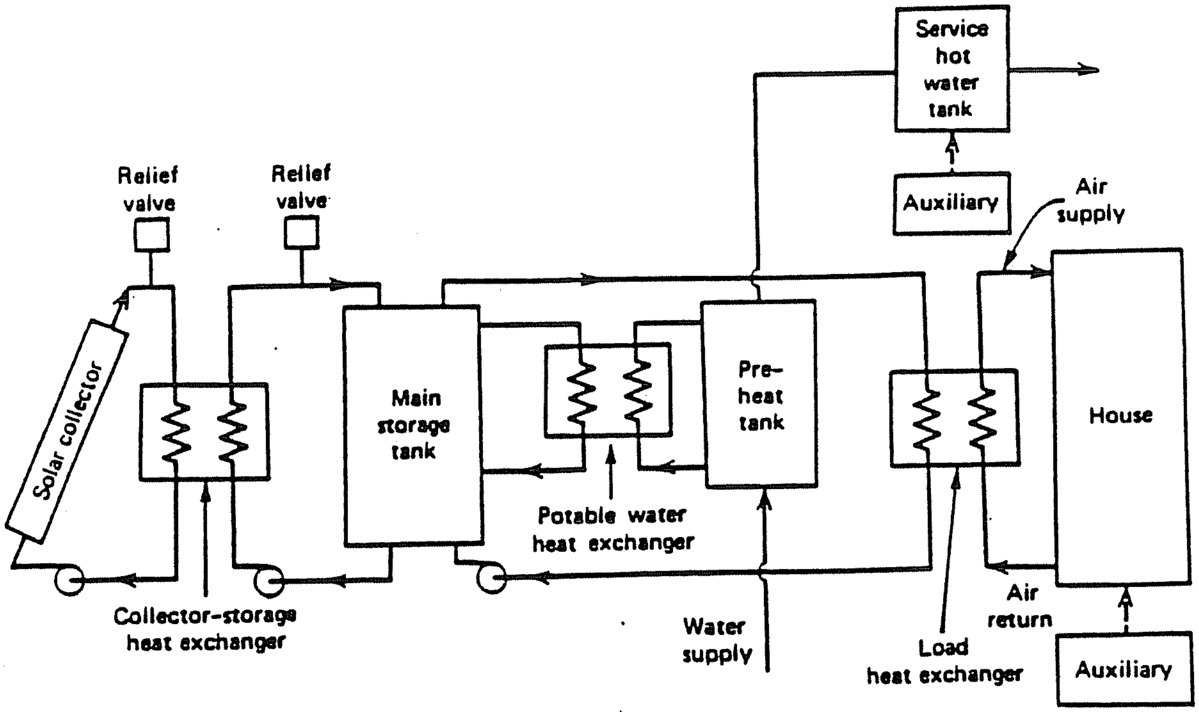

Figure 1. Schematic of the standard system configuration using liquid heat transfer and storage media.

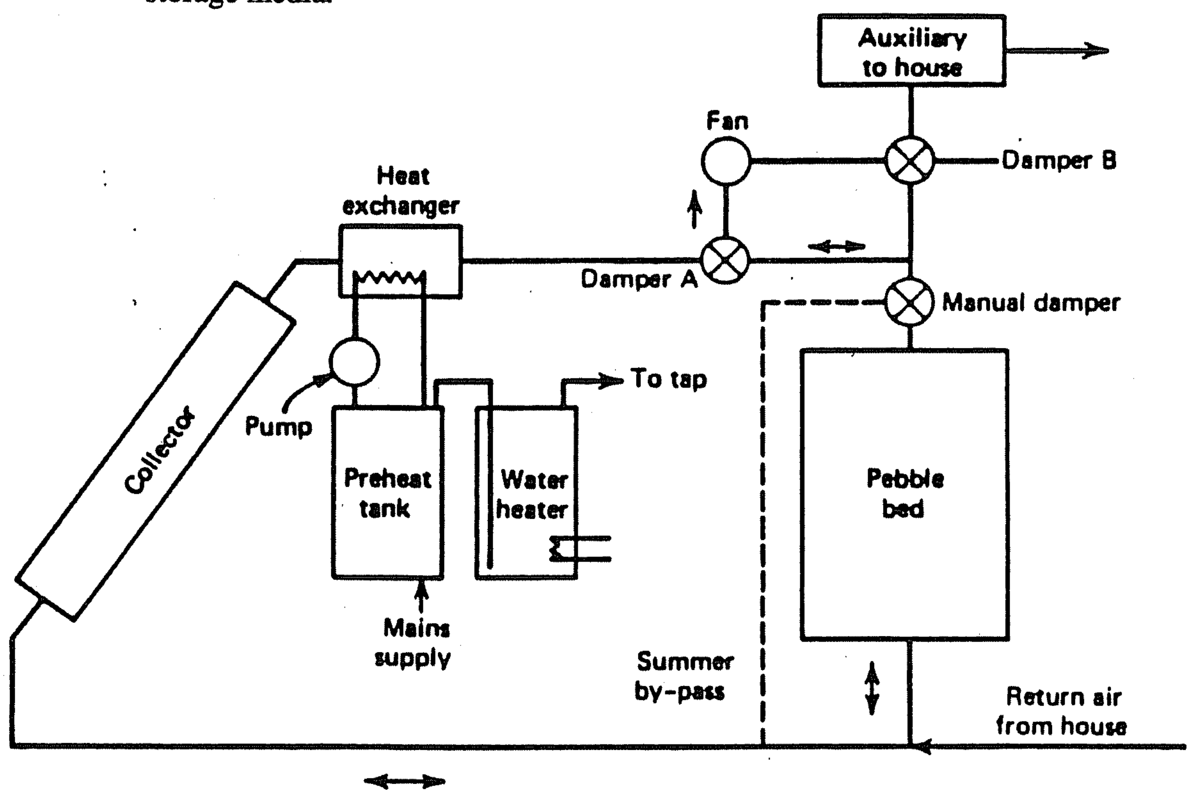

Figure 2. The standard air system configuration.

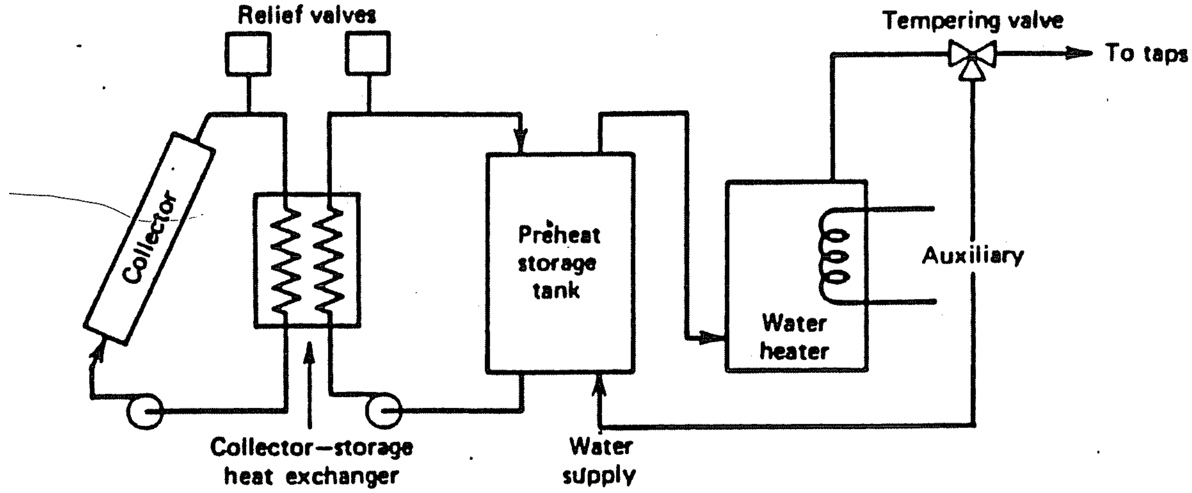

Figure 3. The standard system configuration for water heating only. Collector may heat air or water.

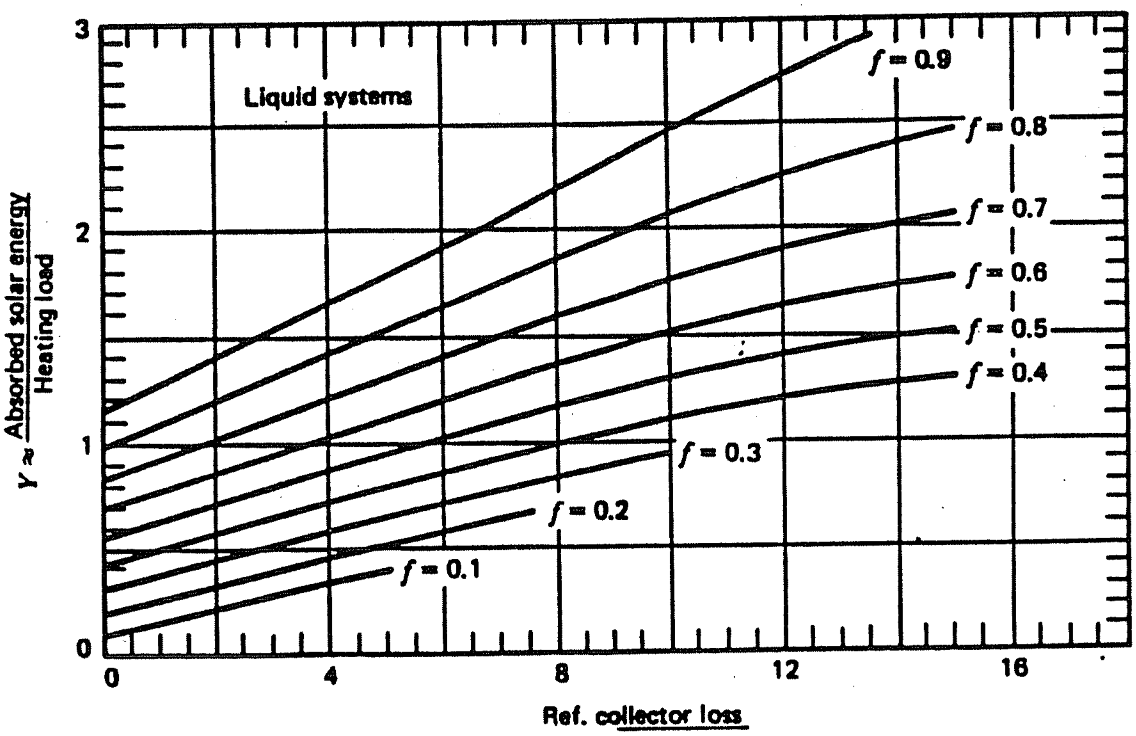

Figure 4. The f-Chart for systems using liquid heat transfer and storage media. From Beckman, et al. (1977).

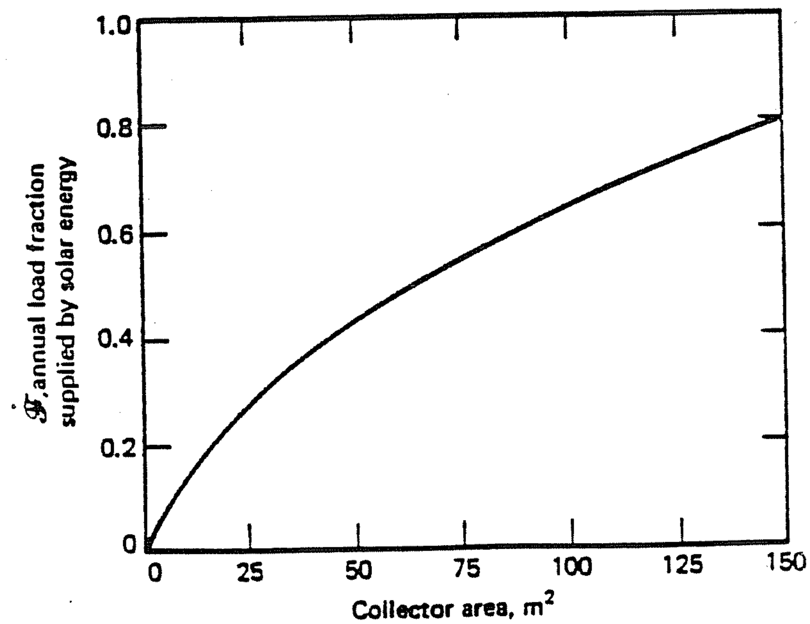

Figure 5. Annual load fraction versus collector area.

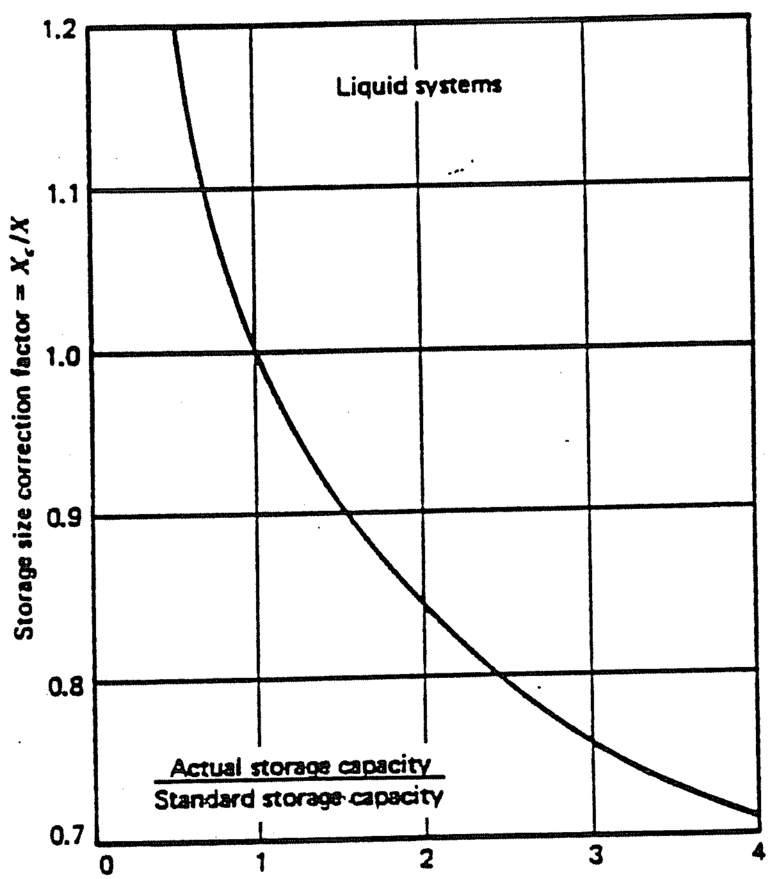

Figure 6. Storage size correction factor for liquid systems. Standard storage capacity is 75 liters/m^2.

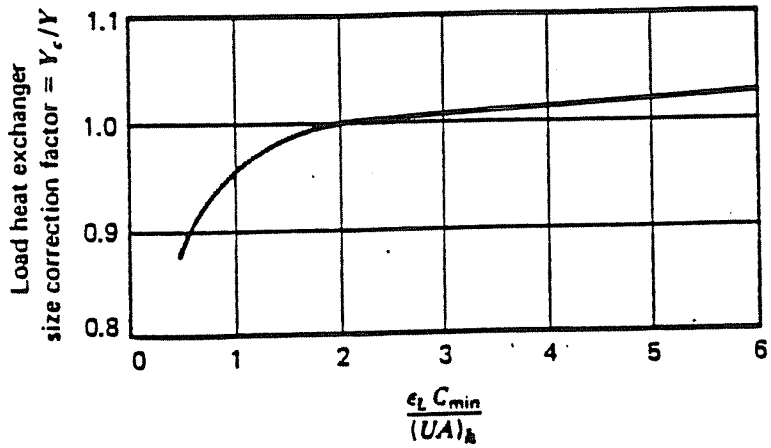

Figure 7. Load heat exchangers size correction factor.

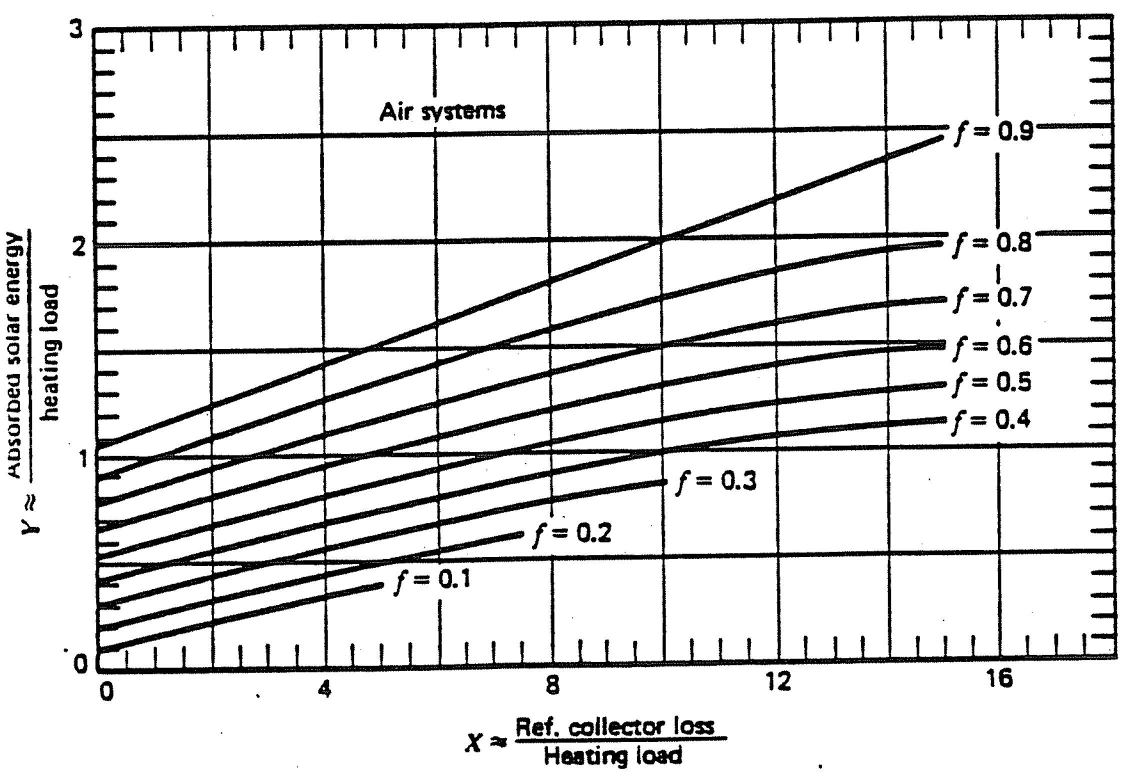

Figure 8. The f-Chart for air systems of the configuration shown in Figure 5. From Beckman, et al. (1977).

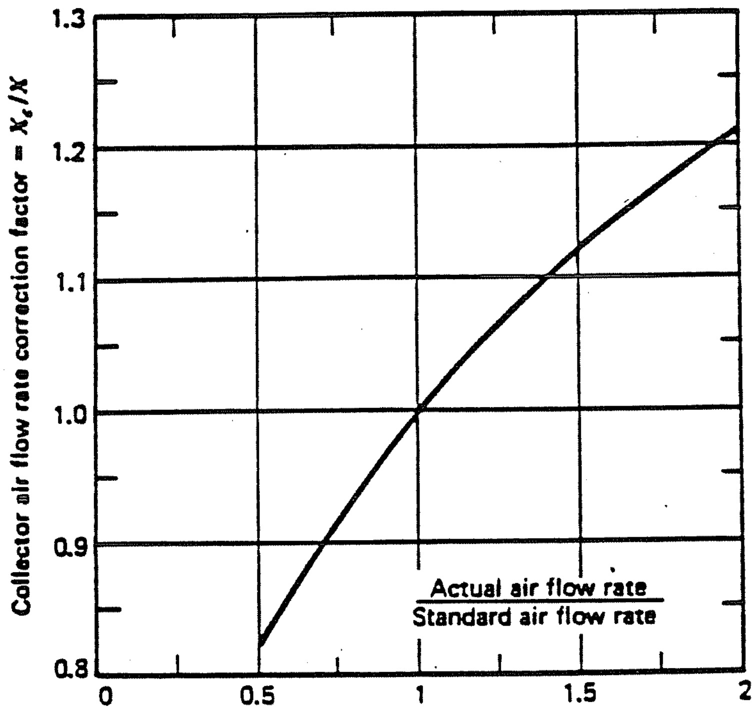

Figure 9. Correction factor for air flowrate to account for stratification in the pebble bed. The standard flowrate is 10 liters/m2s.

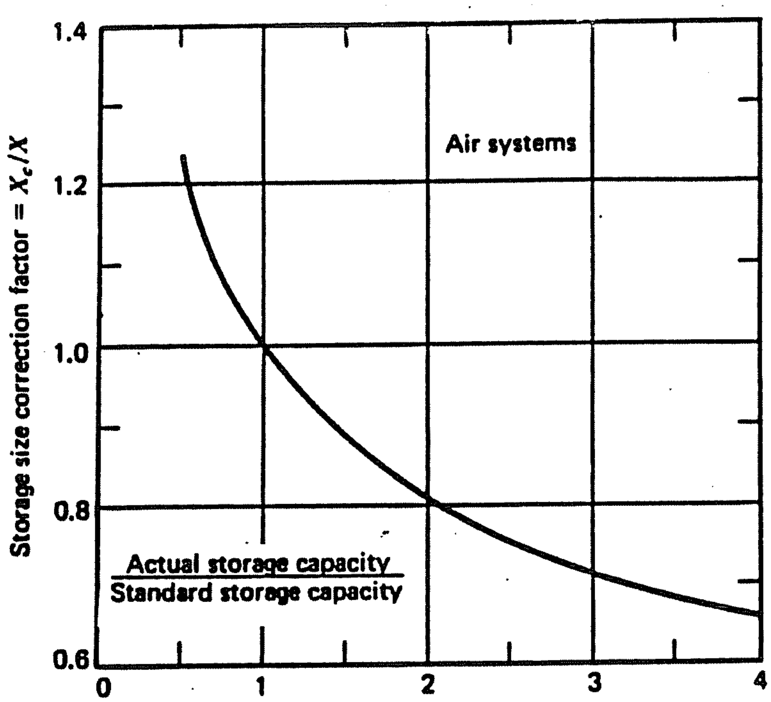

Figure 10. Storage size correction factors for air systems. The standard storage capacity is 0.25 m^3/m^2.

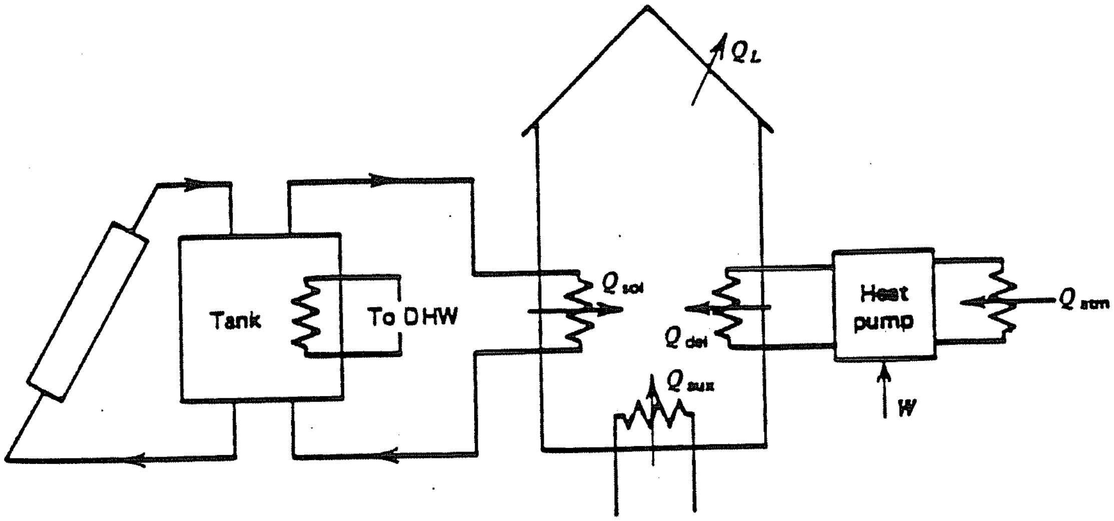

Figure 11. Parallel solar-heat pump system. From Anderson (1979).

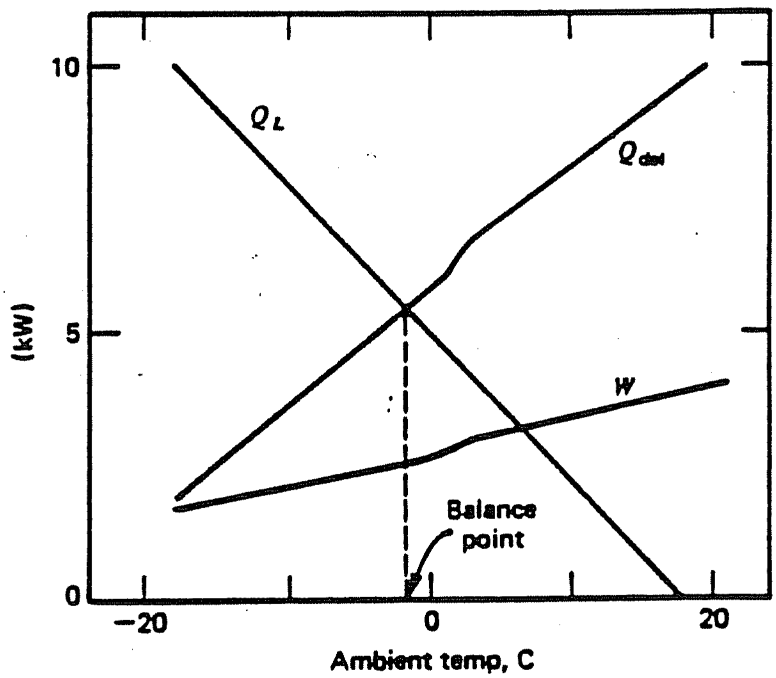

Figure 12. Typical heat pump and load characteristics as a function of ambient temperature. From Anderson (1979).

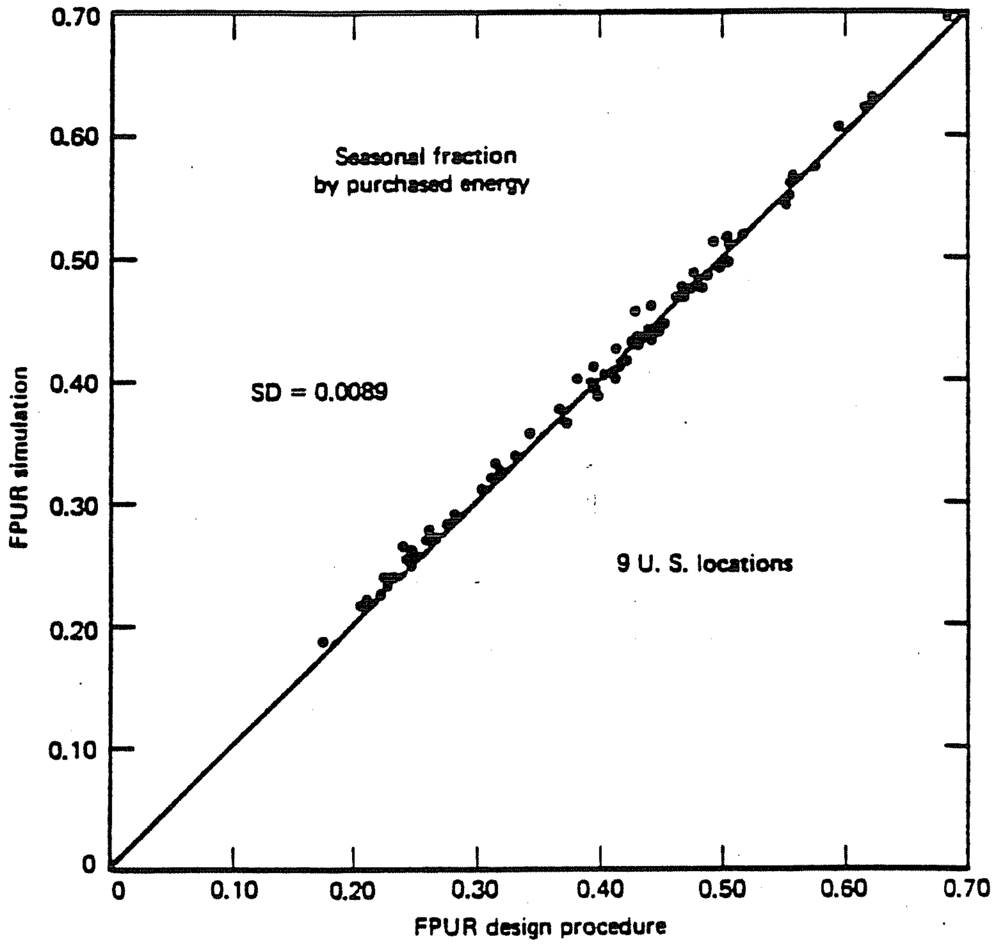

Figure 13. Parallel solar-heat pump system performance for January in Columbia, MO. From Anderson et al. (1970).

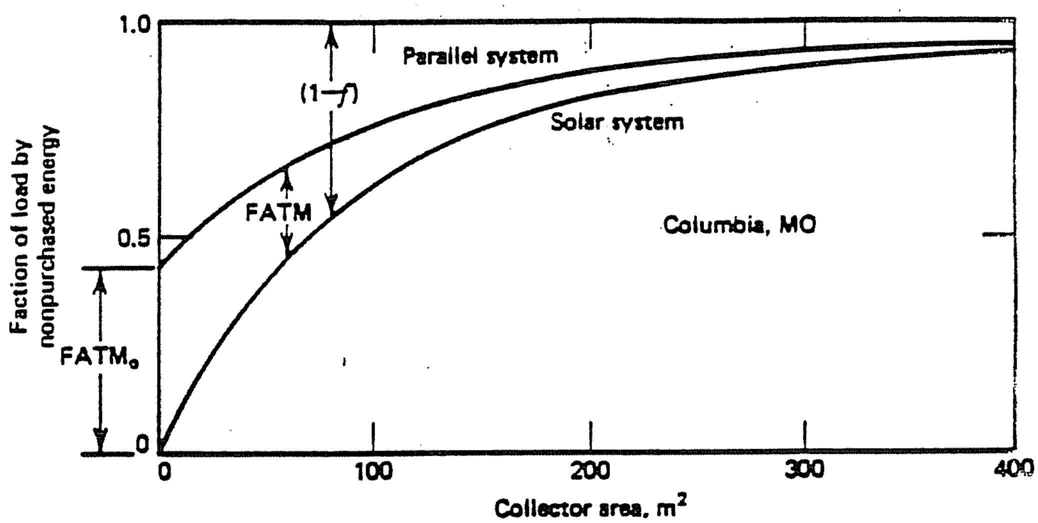

Figure 14. Comparison of purchased energy fractions as calculated by design procedure and by detailed simulations. From Anderson, et al. (1979).